



**Discover Generics**

Cost-Effective CT & MRI Contrast Agents

 **FRESENIUS  
KABI**

[WATCH VIDEO](#)

**AJNR**

## Age-Dependent Normal Values of T2\* and T2 ' in Brain Parenchyma

S. Siemonsen, J. Finsterbusch, J. Matschke, A. Lorenzen,  
X.-Q. Ding and J. Fiehler

*AJNR Am J Neuroradiol* 2008, 29 (5) 950-955

doi: <https://doi.org/10.3174/ajnr.A0951>

<http://www.ajnr.org/content/29/5/950>

This information is current as  
of June 4, 2025.

## ORIGINAL RESEARCH

S. Siemonsen  
J. Finsterbusch  
J. Matschke  
A. Lorenzen  
X.-Q. Ding  
J. Fiehler

# Age-Dependent Normal Values of T2\* and T2' in Brain Parenchyma

**BACKGROUND AND PURPOSE:** Physiologic age-related T2\* and T2' values are required as reference for comparison with disease-related deviations. In our study, T2\* and T2' values (T2 values as control) were determined with MR imaging in healthy subjects to determine standard values and investigate age-related changes.

**MATERIALS AND METHODS:** Data of 50 patients without intraparenchymal pathology and 10 acute stroke patients who underwent MR imaging including a T2 and T2\* sequence with 3 echotimes were included. After calculation of T2\*, T2', and T2 maps, the values of gray matter (GM) and white matter (WM) for each hemisphere were measured in 6 distinct regions of interest (ROIs).

**RESULTS:** There was a negative correlation between age and T2\* values in the caudate nucleus ( $r = -0.34$  Pearson correlation;  $P = .001$ ) and lentiform nucleus ( $r = -0.67$ ;  $P = .001$ ) and a positive correlation in the occipital ( $r = 0.41$ ;  $P = .001$ ) and subcortical ( $r = 0.45$ ;  $P = .001$ ) WM. An age dependency for T2' values was only found for the caudate ( $r = -0.35$ ;  $P = .001$ ) and lentiform nucleus ( $r = -0.69$ ;  $P = .001$ ). T2' values in acute stroke were lower than normal in all patients with stroke.

**CONCLUSION:** Decrease in T2' and T2\* values in GM and increase of T2\* values in WM correlate with the progress of brain aging. Explanations for decreasing T2' and T2\* values include iron deposition in the caudate and lentiform nucleus. In contrast to T2\* values, there is no association of T2' values with the degree of leukoaraiosis. These age-dependent values can be used as a reference in neurovascular diseases and for the discussion of functional MR imaging data.

The possibility of measurements of T2\* and T2' values is of considerable interest for the application of MR imaging in the evaluation of cerebral disease. The use of quantitative techniques potentially increases the diagnostic sensitivity and specificity in the characterization of brain tissue pathologic processes. T2\* and T2' values represent intrinsic parameters of tissue that determine MR imaging signal intensity. These values are sensitive to changes in chemical composition and metabolic modifications that accompany cerebral pathologic processes. T2' is equal to T2\* corrected for spin-spin effects and therefore better isolates the influences of deoxyhemoglobin on T2\* values according to the formula  $1/T2' = 1/T2^* - 1/T2$ .<sup>1,2</sup>

Quantitative MR values have been used in several studies for different conditions. Measurement of T2 values is used in the diagnosis of leukoencephalopathy or developmental anomalies of gray (GM) and white matter (WM) in children.<sup>3</sup> It has been known for a long time that age-dependent changes in brain structure and metabolism are associated with changes of relaxation values.<sup>4</sup> Measurement of T2\* and T2' values has been used for determination of iron tissue concentration,<sup>5</sup> and calculation of T2' values has already been used in MR imaging in acute stroke to investigate the oxygen extraction fraction (OEF) in acute ischemic stroke<sup>2,6</sup> and chronic misery perfusion.<sup>7,8</sup> However, normal reference T2' values have not been reported so far, and the determination of T2' reference values

is mandatory for future applications in ischemic disease. In our study, T2\* and T2' values (and T2 values as control) were determined with MR imaging in distinct regions of interest (ROIs) in the WM and in the basal ganglia in subjects without intraparenchymal pathologic processes to determine age-related normal values. To prove applicability of the obtained T2' normal values, in addition, T2' values were measured in 10 patients with acute stroke.

## Patients and Methods

Fifty patients were retrospectively selected from a pool of 220 consecutive patients who underwent routine MR imaging examination, including a T2 and T2\* sequence with 3 different echotimes (TE) and calculation of corresponding T2' maps in our department between August 2006 and January 2007. Informed consent on the use of their data for study purposes was obtained from all persons included. Only subjects without intraparenchymal pathologic processes as determined independently by 2 experienced neuroradiologists were included. Leukoaraiosis was considered a regular aging process and was graded corresponding to the Fazekas score.<sup>9</sup> Patients with any other brain lesions (eg, brain tumors or other structural defects) were excluded.

## MR Imaging Protocol and T2 Maps

All MR imaging scans were conducted on a 1.5T MR system (Magnetom Sonata; Siemens, Erlangen, Germany). The MR protocol included a T2 and T2\* sequence. For T2 determination, a fast spin-echo sequence with 15 echoes per shot was used to acquire images at 3 different TE of 12, 84, and 156 ms within a total acquisition time of 74 s (number of sections, 24; section thickness, 5 mm; section spacing, 0 mm; FOV, 240 mm; matrix, 74 × 128; TR, 4550 ms; and refocusing flip angle, 150°). T2\*-weighted images were obtained with a single-shot echo-planar imaging sequence at a TE of 20, 52, and 88 ms and a TR of 3240 ms, giving a total acquisition time of 19 s (flip angle, 90°; other parameter as for T2).

Received October 9, 2007; accepted after revision November 22.

From the Departments of Neuroradiology (S.S., A.L., J. Fiehler) and Systems Neuroscience (J. Finsterbusch), and Institute of Neuropathology (J.M.), University Medical Center Hamburg-Eppendorf, Hamburg, Germany; and Institute of Diagnostic and Interventional Neuro-radiology (X.-Q.D.), Medical University Hannover, Germany.

This study was supported by the European Union (Proposal/Contract 027294-I-Know-STREP).

Please address correspondence to Susanne Siemonsen, Department of Neuroradiology, University Medical Center Hamburg-Eppendorf, Martinistr 52, 20246 Hamburg, Germany; e-mail: s.siemonsen@uke.uni-hamburg.de

DOI 10.3174/ajnr.A0951

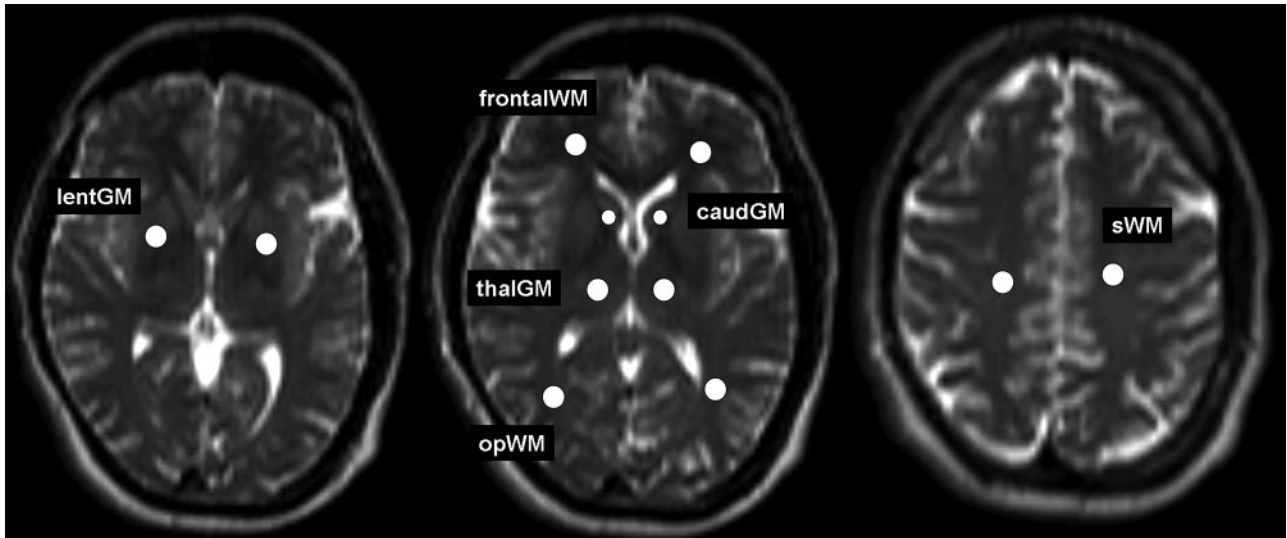


**Fig 1.** Definition of 6 ROIs on T2-weighted images chosen in different brain regions: frontal WM (*frontalWM*), occipitoparietal WM (*opWM*), subcortical WM (*sWM*), caudate nucleus (*caudGM*), thalamus (*thalGM*), and lentiform nucleus (*lentGM*).

### Calculation of $qT2^*$ , $qT2'$ and $qT2$ Images

Quantitative T2 ( $qT2$ ),  $qT2^*$ , and  $qT2'$  maps were obtained on-the-fly on the MR system with an extended image reconstruction algorithm custom made by the manufacturer's image calculation environment (ICE).  $T2^*$  and T2 maps were calculated by separately fitting a single exponential term to the signal intensity decay curve given by  $SI(t) = SI_0 e^{-t/T2}$  for the signal intensities of the multiple TE data ( $SI(t)$ ) of the T2 and  $T2^*$  sequences.  $T2'$  is equivalent to  $T2^*$  corrected for spin-spin ( $T2$ ) effects according to the relationship:  $1/T2' = 1/T2^* - 1/T2$ .<sup>1</sup> For each voxel, the quantitative T2 and  $T2^*$  values were used to generate  $T2'$  values by applying this relationship.<sup>2</sup> Voxel sizes of the obtained parameter maps were  $3.2 \times 1.9 \times 5 \text{ mm}^3$ .

### Regions-of-Interest Analysis

$T2'$ ,  $T2^*$ , and T2 values of GM and WM were measured in 12 distinctive ROIs on each of the created  $qT2'$ ,  $qT2^*$ , and  $qT2$  maps with medical image processing, analysis, and visualization (MIPAV) software (Center for Information Technology, National Institutes of Health, Bethesda, Md).

For definition of ROIs, T2-weighted images (third echo of triple-echo T2 sequence) were used. Predefined ROIs were then transferred to corresponding  $qT2'$ ,  $qT2^*$ , and  $qT2$  images.

$T2^*$ ,  $T2'$ , and T2 values of deep GM and WM for each hemisphere were measured in 6 ROIs chosen in different brain regions: frontal WM (*frontalWM*), occipitoparietal WM (*opWM*), subcortical WM (*sWM*), caudate nucleus (*caudGM*), thalamus (*thalGM*), and lentiform nucleus (*lentGM*) (Fig 1). For definition of the first 2 GM ROIs, the same transaxial section was used. The third ROI was located in the axial section showing the largest extent of the transaxial sectioned lentiform nucleus. The ROIs were chosen carefully to minimize partial volume effects. All ROIs were the same shape and comprised an area of  $21 \text{ mm}^2$ , except for the ROI at the caudate nucleus, which was chosen with an area of  $12 \text{ mm}^2$ . These 2 types of ROIs were predefined manually and then transferred for each patient intraindividually to each parameter map. No ROIs were chosen in cortical GM because of substantial partial volume effects contributed by CSF. We conducted all numeric calculations for ROI analysis using the MIPAV software. Statistical analysis was performed with SPSS 13.0 (correlation between grade of leukoaraiosis and T2,  $T2^*$ , and  $T2'$  WM values [Spearman rho]; cal-

culatation of Pearson correlation coefficients and corresponding  $P$  values for each ROI localization and the age dependence of  $T2^*$ ,  $T2'$ , and T2 values; and Mann-Whitney  $U$  test for comparison of  $T2'$  values measured in patients with acute stroke with normal reference value).

### Measurement of $T2'$ Values in Acute Stroke Lesions

For proof of principle,  $T2'$  values were measured within the hypoperfused brain tissue in 10 patients with acute stroke. Inclusion criteria were MR imaging examination within 6 hours after the onset of symptoms; acute ischemic stroke in the territory of the middle cerebral artery; and visible, hypointense lesion on  $T2'$  maps in WM of the affected hemisphere. Hypoperfused tissue was delineated in time-to-peak perfusion maps as the region with perfusion delay apparent for the observer by visual inspection. Mean  $T2'$  values were obtained for each patient.

### Results

The mean age of the patients was  $54 \pm 20$  years (mean  $\pm$  SD) ranging from 12 to 91 years (30 male and 20 female). Age distribution for the entire collective was found as illustrated in Fig 2.

$T2'$ ,  $T2^*$ , and T2 values were determined for all 50 patients within 6 ROIs for each hemisphere. Mean absolute values and SD for  $T2^*$ ,  $T2'$ , and T2 values are listed in Table 1.

Mean T2,  $T2^*$ , and  $T2'$  values for WM corresponding to different grades of leukoaraiosis are displayed in Table 2. A significant correlation was observed between the grade of leukoaraiosis and T2 WM values (Spearman rho  $\rho = 0.293$ ;  $P < .001$  [2-tailed]) and also with  $T2^*$  WM values (Spearman rho  $\rho = 0.215$ ;  $P < .001$  [2-tailed]). No significant correlation was found for  $T2'$  values measured in WM ROIs.

Correlation coefficients and corresponding  $P$  values for each ROI localization and the age dependence of  $T2^*$ ,  $T2'$ , and T2 values are displayed in Table 3.

In addition, age-related changes in  $T2^*$ ,  $T2'$ , and T2 values were determined for male ( $n = 30$ ; mean age, 54 years; minimum, 15 years; maximum, 78 years) and female ( $n = 20$ ; mean age, 54 years; minimum, 12 years; maximum, 91 years) patients separately. Even stronger correlation coefficients were observed compared with analysis of the entire patient collective when data of the female patient group were separately

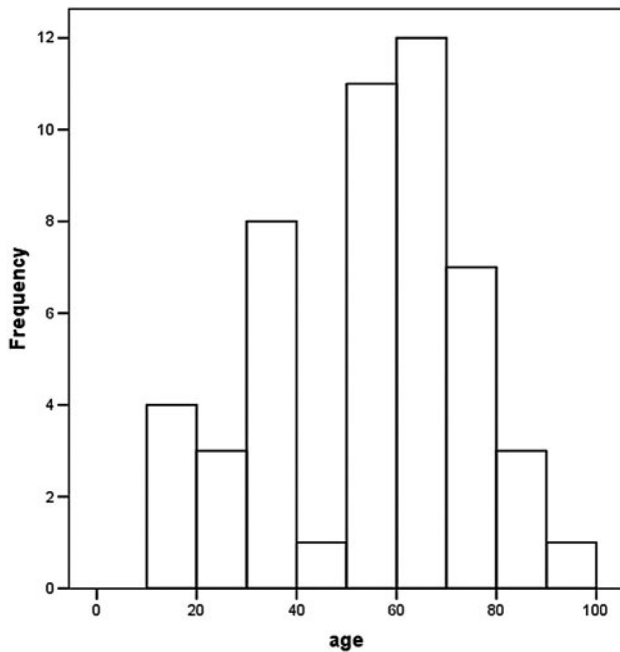


Fig 2. Age distribution of the healthy subjects.

Table 1: Mean (MW) and SD for T2\*, T2', and T2 values

Values	MW (ms)	SD
T2*_GM	48.48	12.09
T2*_WM	67.63	11.01
T2_GM	96.07	9.06
T2_WM	109.77	11.37
T2'_GM	109.92	44.91
T2'_WM	170.47	99.26

Note:—GM indicates gray matter; WM, white matter.

Table 2: Mean (MW) and SD for T2\*, T2, and T2' values for WM corresponding to different grades of leukoaraiosis (0–6)

WM Values	Leukoaraiosis		MW (ms)	SD
	Grade			
T2* WM	0		66.12	8.19
	1		68.21	10.65
	2		67.10	10.48
	3		74.54	8.60
	4		64.25	27.78
	5		70.74	20.20
	6		69.56	18.61
T2 WM	0		105.97	10.00
	1		111.46	11.18
	2		109.27	10.12
	3		114.11	11.01
	4		123.75	11.48
	5		124.13	15.46
	6		119.44	9.14
T2' WM	0		161.07	76.12
	1		173.19	110.79
	2		169.98	91.62
	3		219.38	160.68
	4		147.58	124.84
	5		158.31	96.44
	6		181.26	118.54

Note:—WM indicates white matter.

analyzed. In addition, there was a significant positive correlation between age and T2' values in the occipital WM ( $r = 0.42$ ;

Table 3: Pearson correlation coefficients and corresponding P values for each ROI localization and the age dependence of T2\*, T2', and T2 values

T2 Values, ROI Localization	Pearson Correlation Coefficient	P Value
T2*_caudGM	−0.34	.001*
T2*_lentGM	−0.67	.001*
T2*_thalGM	0.10	.336
T2*_frontalWM	−0.01	.933
T2*_opWM	0.41	.001*
T2*_sWM	0.45	.001*
T2_caudGM	−0.18	.067
T2_lentGM	−0.14	.168
T2_thalGM	0.55	.001*
T2_frontalWM	0.60	.001*
T2_opWM	0.42	.001*
T2_sWM	0.65	.001*
T2'_caudGM	−0.35	.001*
T2'_lentGM	−0.69	.001*
T2'_thalGM	−0.13	.200
T2'_frontalWM	0.00	.995
T2'_opWM	0.19	.053
T2'_sWM	0.01	.920

Note:—ROI indicates region of interest; GM, gray matter; WM, white matter; opWM, occipitoparietal WM; sWM, subcortical WM; caudGM, caudate nucleus; thalGM, thalamus; and lentGM, lentiform nucleus.

\* Indicating significant correlation (2-tailed).

$P \leq .001$ ) and a significant negative correlation between age and T2 in the caudate nucleus ( $r = -0.37$ ;  $P \leq .001$ ) for the female group. In contrast to the results for the entire patient collective, the male patient group did not show significant ( $P \leq .001$ ) correlation between age and values determined in the caudate nucleus on T2\* and T2' maps as well as in occipital WM on T2\* images. There was no significant sex- or side-dependent difference in absolute values of T2, T2\*, or T2'.

### Measurement of T2' Values in Patients With Acute Stroke

Mean T2' values measured in ROIs defined in hypointense lesions in the infarcted hemisphere compared with the above obtained T2' normal value for WM of 170.47 ms (95% confidence interval, 159.24–181.70 ms) are displayed in Fig 3. All T2' values measured in patients with acute stroke inside the visible hypointense T2' lesion were lower than the obtained normal reference value for WM in healthy control subjects ( $P < .001$ ).

### Discussion

Quantitative MR techniques have been shown to be sensitive to microstructural and metabolic changes.<sup>3,10</sup> The use of quantitative MR imaging parameters such as T2\*, T2', and T2 values, each contributing to different tissue characteristics, is essential to detect alterations in signal intensity resulting from tissue abnormalities. Reference values of healthy control subjects with respect to age are essential to interpret the observed values in pathologic conditions. Therefore, we sought to investigate T2\* and T2' values in healthy control subjects and their age-related changes. Absolute T2 values and their age-related changes have been investigated by several studies.<sup>3,11–13</sup> In our study, T2 values were determined as controls in addition to the primary target variables T2\* and T2' parameters. The mean T2 value of 170 ms for WM in our study agrees with a study reporting a T2 value of 96 ms in WM obtained in the

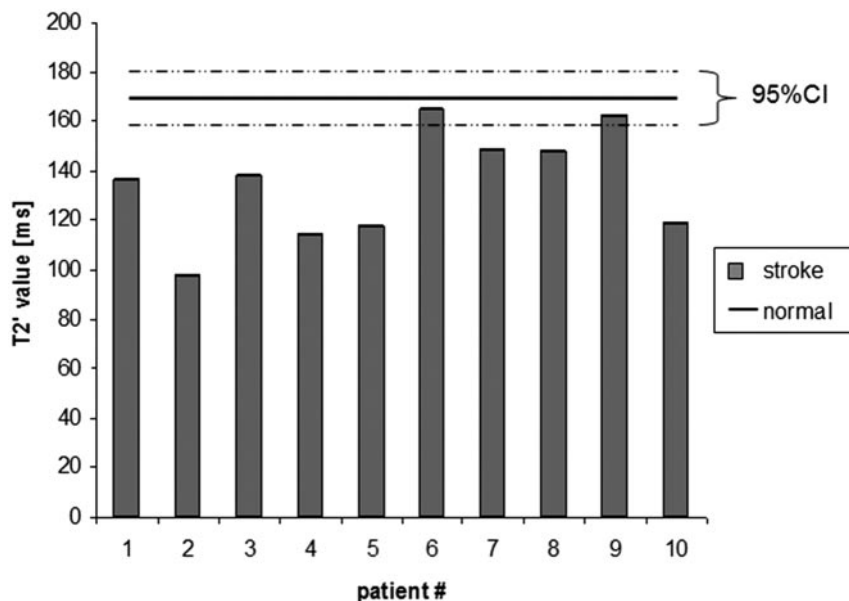


**Fig 3.** T2' values measured in acute stroke lesion (*stroke*) compared with normal reference values in healthy subjects (*normal*).

on T2\* weighted BOLD MR imaging are dependent on changes in the local concentration of deoxyhemoglobin.<sup>19</sup> A hypointense lesion on BOLD imaging corresponding to a decrease of T2\* indicates an increased local deoxyhemoglobin concentration. Thus, T2\* changes reflect an alteration in oxygen availability and might be related to age.<sup>2,20</sup> The BOLD effect is superimposed on the underlying T2 processes in determining T2\*. Therefore, separation of these 2 contributions better isolates the influences of deoxyhemoglobin on T2\*. The T2' image more clearly displays susceptibility related influences of deoxyhemoglobin on T2\*.

temporal lobe of adults,<sup>14</sup> and another study, describing a T2 value of 95 ms for frontoparietal WM.<sup>15</sup> Other studies<sup>11</sup> have found a significant effect of age on T2 values in WM and also a positive effect on T2 values in the thalamus with aging. T2' values were independent from pre-existing leukoaraiosis.

Obtaining normal values for T2' as a reference is equally essential because T2' maps have already been used in several studies to measure the OEF as a parameter of brain metabolism, especially in vascular pathologic processes such as arterial stenosis and stroke.<sup>6,16</sup> Positron-emission tomography (PET) is usually needed to measure the OEF.<sup>17</sup> In contrast, T2' maps are more easily applicable in clinical routine and can easily be incorporated into an protocol for acute stroke. Normal reference values are needed to allow further evaluation of pathologic variation in brain tissue. To our knowledge, there are no studies reporting on normal T2' values as a reference so far. In our study, mean T2' values in WM were 170 ( $\pm$  99 SD) and 109.92 ( $\pm$  44.91 SD) in GM. These values show a high SD and variance compared with T2\* and T2 values (Table 1). This shortcoming is easily understood when considering the formula  $1/T2^* - 1/T2 = 1/T2'$ ,<sup>2</sup> implying that small changes in T2 or T2\* values show, in contrast, a large effect on T2' values. The acquisition of the T2' sequence still needs improvement, but in the setting of acute stroke, time limitations prohibit achieving a better signal-to-noise ratio at the cost of acquisition time.

Moreover, the results have implications with regard to functional MR imaging studies because blood oxygen level-dependent (BOLD) optimization in signal intensity is achieved when TEs are set equal to the T2\* values of the tissue of interest. The magnitude of the BOLD change in signal intensity on brain functional MR imaging is dependent on intrinsic tissue properties such as transverse relaxation time (T2\*) and extrinsic parameters such as TE and magnetic field strength.<sup>18</sup> In addition, abnormalities shown with these techniques may correspond to increasing calcification in areas of the extrapyramidal system or, in cases of T2' images, to a variation in the deoxyhemoglobin concentration as an indicator of the OEF in brain parenchyma. Changes in signal intensity

To demonstrate applicability of the obtained T2' normal values, in addition, T2' values were measured in 10 patients with acute stroke. PET studies reported an increase of the OEF in ischemic brain tissue. Similar to hyperacute ischemic lesions in CT, the regions with abnormalities on T2' BOLD imaging are clearly visible to the human eye, and a measurable loss of T2' signal intensity in the infarcted hemisphere compared with the unaffected hemisphere has been reported.<sup>6</sup> Our observations are in line with these reports. The T2' values for all 10 patients with acute stroke were significantly lower ( $P < .001$ ) than the T2' normal value of 170 ms.

Age-related changes in brain anatomy during human development represent one of the most challenging and important topics of research in neuroscience. During infancy and adolescence, developmental changes occur in GM and WM microstructure and organization of the brain.<sup>21,22</sup> MR imaging has mainly contributed to the understanding of age-related brain changes, providing a noninvasive tool to study the normal aging process in vivo at multiple time points<sup>23-26</sup> because it is highly sensitive for detecting abnormalities of signal intensity in brain parenchyma leading to increased recognition of alterations in signal intensity of the WM. Most of these WM lesions generally appear as hyperintense on T2-weighted images. Various studies describe a relationship between these hyperintensities and increasing age.<sup>27-30</sup> In this context, it has been shown that T2 parameters do not provide sufficient information about the underlying microstructural modifications of brain tissue occurring with aging because they are affected by several factors such as tissue attenuation and tissue water content as well as by iron content in the tissue.<sup>5,31</sup>

Having obtained the individual T2\*, T2', and T2 values for all subjects, we studied the age dependence of T2\*, T2', and T2 values. The accumulation of paramagnetic metals such as iron could be a main reason for the reduction of the T2\*, T2', and T2 values in deeper GM<sup>32</sup> as it was also observed in our study. The normal aging changes of the brain include enlargement of the sulci and ventricles, and focal changes in WM.<sup>22,33,34</sup> Our results suggest an overall tendency for increase in T2\*, T2, and T2' during the aging process. In particular, dynamic degenerative changes of the microstructure in brain parenchyma be-

cause of leukoaraiosis might contribute mainly to the detected increase of T2\* and T2, especially in the WM. However, there was no association of T2' values with leukoaraiosis in our patients. Histopathologic studies have revealed that WM hyperintensities are associated with areas of tissue destruction in demyelination and axonal changes such as a reduction of the total length of myelinated fibers and also fiber loss, and that these reported changes are detectable with quantitative MR imaging techniques.<sup>35-37</sup> The increase in T2\* and T2 values with age could represent diffuse structural changes in neurons or myelin or a decrease in the cellularity of the brain with aging. In the alternative sense, the reported increase in measured values may reflect small focal abnormalities not visualized with MR imaging, such as senile plaques, amyloid deposits, small infarcts, or Virchow-Robin spaces.<sup>33</sup>

Basal ganglia represent an area especially susceptible to pathophysiologic processes associated with deposition of iron resulting in changes in signal intensity on MR imaging of the individual brain with older age.<sup>38,39</sup> MR imaging sequences such as T2\* and T2' are highly sensitive to ferritin iron within brain tissue. In clinical practice, increased iron deposits may be visible by darkening of the basal ganglia on qT2\*, qT2', and qT2 maps.<sup>37</sup> Visualizing normal iron deposition as detected with MR imaging might be helpful in the diagnosis of known iron-deposition diseases and also in the detection of iron-related pathologic changes. Because the increase in iron in the brain is age related, the role of iron in age-related neurodegenerative disorders still needs investigation.<sup>31,39</sup> Age-related changes in signal intensity from the pallidum or thalamus, possibly attributable to the deposition of iron, have been reported.<sup>22</sup> Rivkin et al<sup>40</sup> measured T2\* values in brain tissue of neonates and adults with a mean age of 38 years, which included the frontal and parietooccipital areas in the WM as well as the thalamus. For the adult group, they reported mean T2\* values ranging from 62 to 69 ms and a brain average of T2\* values of 66 ± 5 ms. The T2\* values we obtained in corresponding ROIs are in line with these measurements and are also consistent with those reported by Speck et al.<sup>8</sup>

In theory, the more echoes, and thus more points, for calculation of the signal intensity decay curve would be beneficial for the derivation of T2 and T2\* values and, consecutively, of T2' values than from triple-echo sequences. In clinical routine, though, multi-echo MR images with more echoes also require a longer TR. This leads to a longer MR acquisition time and higher sensitivity to artifacts from patient movement, which is most relevant in patients with acute stroke. Another reason for deviations of measured values compared with other studies might be that ferritin has been observed to exert a strong magnetic effect that results in marked T2 shortening,<sup>41-43</sup> and tissue T2 parameters have been shown to be field dependent.<sup>44,45</sup> Ferritin itself shortens T2 more in high-field than in low-field instruments.<sup>31,46</sup> Hence, cerebral T2 values decrease with increasing field strength,<sup>5</sup> and several qT2 reference values were obtained by low-field systems.<sup>3,12,47</sup>

Most of the patients included in our study presented with a variety of neurologic symptoms because only patients with an indication for MR imaging examination were scanned. None of the subjects included in our study showed pathologic changes in brain tissue. Because information concerning demographic factors such as race, lifestyle factors such as alcohol

and coffee consumption, and medical history factors such as surgery and drug use was not available, we are not able to determine whether these might contribute to our results.

## Conclusions

Decrease in T2' and T2\* relaxation time values in GM and increase of T2\* and T2 in WM correlate with the progress of the aging brain. We hypothesize that decreasing T2' and T2\* values result from iron deposition in the caudate and lenticular nucleus, whereas the increase in WM may be related to an increased OEF. In contrast to T2\* values, there is no association of T2' values with the degree of leukoaraiosis. These age-dependent values can be used as a reference in neurovascular diseases and for the discussion of functional MR imaging data.

## References

- Calamante F, Lythgoe MF, Pell GS, et al. Early changes in water diffusion, perfusion, T1, and T2 during focal cerebral ischemia in the rat studied at 8.5 T. *Magn Reson Med* 1999;41:479-85
- An H, Lin W. Quantitative measurements of cerebral blood oxygen saturation using magnetic resonance imaging. *J Cereb Blood Flow Metab* 2000;20:1225-36
- Ding XQ, Kucinski T, Wittkugel O, et al. Normal brain maturation characterized with age-related T2 relaxation times: an attempt to develop a quantitative imaging measure for clinical use. *Invest Radiol* 2004;39:740-46
- Bottomley PA, Foster TH, Argersinger RE, et al. A review of normal tissue hydrogen NMR relaxation times and relaxation mechanisms from 1-100 MHz: dependence on tissue type, NMR frequency, temperature, species, excitation, and age. *Med Phys* 1984;11:425-48
- Brooks DJ, Luthert P, Gadian D, et al. Does signal-attenuation on high-field T2-weighted MRI of the brain reflect regional cerebral iron deposition? Observations on the relationship between regional cerebral water proton T2 values and iron levels. *J Neurol Neurosurg Psychiatry* 1989;52:108-11
- Geisler BS, Brandhoff F, Fiehler J, et al. Blood-oxygen-level-dependent MRI allows metabolic description of tissue at risk in acute stroke patients. *Stroke* 2006;37:1778-84
- Speck O, Chang L, DeSilva NM, et al. Perfusion MRI of the human brain with dynamic susceptibility contrast: gradient-echo versus spin-echo techniques. *J Magn Reson Imaging* 2000;12:381-87
- Speck O, Ernst T, Chang L. Biexponential modeling of multigradient-echo MRI data of the brain. *Magn Reson Med* 2001;45:1116-21
- Fazekas F, Chawluk JB, Alavi A, et al. MR signal abnormalities at 1.5 T in Alzheimer's dementia and normal aging. *AJR Am J Roentgenol* 1987;149:351-56
- Inglese M, Ge Y. Quantitative MRI: hidden age-related changes in brain tissue. *Top Magn Reson Imaging* 2004;15:355-63
- Breger RK, Yetkin FZ, Fischer ME, et al. T1 and T2 in the cerebrum: correlation with age, gender, and demographic factors. *Radiology* 1991;181:545-47
- Agartz I, Saaf J, Wahlund LO, et al. T1 and T2 relaxation time estimates in the normal human brain. *Radiology* 1991;181:537-43
- Fan G, Wu Z, Pan S, et al. Quantitative study of MR T1 and T2 relaxation times and IHMRS in gray matter of normal adult brain. *Chin Med J (Engl)* 2003;116:400-04
- Okujava M, Schulz R, Ebner A, et al. Measurement of temporal lobe T2 relaxation times using a routine diagnostic MR imaging protocol in epilepsy. *Epilepsy Res* 2002;48:131-42
- Dezortova M, Hajek M, Tintera J, et al. MR in phenylketonuria-related brain lesions. *Acta Radiol* 2001;42:459-66
- Tamura H, Hatazawa J, Toyoshima H, et al. Detection of deoxygenation-related signal change in acute ischemic stroke patients by T2\*-weighted magnetic resonance imaging. *Stroke* 2002;33:967-71
- Baron JC, Boussier MG, Comar D, et al. Noninvasive tomographic study of cerebral blood flow and oxygen metabolism in vivo. Potentials, limitations, and clinical applications in cerebral ischemic disorders. *Eur Neurol* 1981;20:273-84
- Bandettini PA, Wong EC, Jesmanowicz A, et al. Spin-echo and gradient-echo EPI of human brain activation using BOLD contrast: a comparative study at 1.5 T. *NMR Biomed* 1994;7:12-20
- Ogawa S, Menon RS, Tank DW, et al. Functional brain mapping by blood oxygenation level-dependent contrast magnetic resonance imaging. A comparison of signal characteristics with a biophysical model. *Biophys J* 1993;64:803-12
- Lee JM, Vo KD, An H, et al. Magnetic resonance cerebral metabolic rate of oxygen utilization in hyperacute stroke patients. *Ann Neurol* 2003;53:227-32

21. Akiyama H, Meyer JS, Mortel KF, et al. **Normal human aging: factors contributing to cerebral atrophy.** *J Neurol Sci* 1997;152:39–49
22. Drayer BP. **Imaging of the aging brain. Part I. Normal findings.** *Radiology* 1988;166:785–96
23. Anderson VC, Litvack ZN, Kaye JA. **Magnetic resonance approaches to brain aging and Alzheimer disease-associated neuropathology.** *Top Magn Reson Imaging* 2005;16:439–52
24. Autti T, Raininko R, Vanhanen SL, et al. **MRI of the normal brain from early childhood to middle age. II. Age dependence of signal intensity changes on T2-weighted images.** *Neuroradiology* 1994;36:649–51
25. Benedetti B, Charil A, Rovaris M, et al. **Influence of aging on brain gray and white matter changes assessed by conventional, MT, and DT MRI.** *Neurology* 2006;66:535–39
26. Evans AC. **The NIH MRI study of normal brain development.** *Neuroimage* 2006;30:184–202
27. Breteler MM, van Swieten JC, Bots ML, et al. **Cerebral white matter lesions, vascular risk factors, and cognitive function in a population-based study: the Rotterdam Study.** *Neurology* 1994;44:1246–52
28. Schmidt R, Fazekas F, Kapeller P, et al. **MRI white matter hyperintensities: three-year follow-up of the Austrian Stroke Prevention Study.** *Neurology* 1999;53:132–39
29. Farkas E, Luiten PG. **Cerebral microvascular pathology in aging and Alzheimer's disease.** *Prog Neurobiol* 2001;64:575–611
30. Fazekas F, Schmidt R, Scheltens P. **Pathophysiologic mechanisms in the development of age-related white matter changes of the brain.** *Dement Geriatr Cogn Disord* 1998;9 Suppl 1:2–5
31. Bartzokis G, Mintz J, Sultzer D, et al. **In vivo MR evaluation of age-related increases in brain iron.** *AJNR Am J Neuroradiol* 1994;15:1129–38
32. Aoki S, Okada Y, Nishimura K, et al. **Normal deposition of brain iron in childhood and adolescence: MR imaging at 1.5 T.** *Radiology* 1989;172:381–85
33. Hendrie HC, Farlow MR, Austrom MG, et al. **Foci of increased T2 signal intensity on brain MR scans of healthy elderly subjects.** *AJNR Am J Neuroradiol* 1989;10:703–07
34. Kirkpatrick JB, Hayman LA. **White-matter lesions in MR imaging of clinically healthy brains of elderly subjects: possible pathologic basis.** *Radiology* 1987;162:509–11
35. Marner L, Nyengaard JR, Tang Y, et al. **Marked loss of myelinated nerve fibers in the human brain with age.** *J Comp Neurol* 2003;462:144–52
36. Aboitiz F, Rodriguez E, Olivares R, et al. **Age-related changes in fibre composition of the human corpus callosum: sex differences.** *Neuroreport* 1996;7:1761–64
37. Kapeller P, Schmidt R, Fazekas F. **Qualitative MRI: evidence of usual aging in the brain.** *Top Magn Reson Imaging* 2004;15:343–47
38. Pujol J, Junque C, Vendrell P, et al. **Biological significance of iron-related magnetic resonance imaging changes in the brain.** *Arch Neurol* 1992;49:711–17
39. Schenker C, Meier D, Wichmann W, et al. **Age distribution and iron dependency of the T2 relaxation time in the globus pallidus and putamen.** *Neuroradiology* 1993;35:119–24
40. Rivkin MJ, Wolraich D, Als H, et al. **Prolonged T\*2 values in newborn versus adult brain: Implications for fMRI studies of newborns.** *Magn Reson Med* 2004;51:1287–91
41. Koenig SH, Brown RD 3rd, Gibson JF, et al. **Relaxometry of ferritin solutions and the influence of the Fe3+ core ions.** *Magn Reson Med* 1986;3:755–67
42. Brittenham GM, Farrell DE, Harris JW, et al. **Magnetic-susceptibility measurement of human iron stores.** *N Engl J Med* 1982;307:1671–75
43. Thulborn KR, Sorensen AG, Kowall NW, et al. **The role of ferritin and hemosiderin in the MR appearance of cerebral hemorrhage: a histopathologic biochemical study in rats.** *AJR Am J Roentgenol* 1990;154:1053–59
44. Dockery SE, Suddarth SA, Johnson GA. **Relaxation measurements at 300 MHz using MR microscopy.** *Magn Reson Med* 1989;11:182–92
45. Vymazal J, Brooks RA, Zak O, et al. **T1 and T2 of ferritin at different field strengths: effect on MRI.** *Magn Reson Med* 1992;27:368–74
46. Bartzokis G, Aravagiri M, Oldendorf WH, et al. **Field dependent transverse relaxation rate increase may be a specific measure of tissue iron stores.** *Magn Reson Med* 1993;29:459–64
47. Michaeli S, Garwood M, Zhu XH, et al. **Proton T2 relaxation study of water, N-acetylaspartate, and creatine in human brain using Hahn and Carr-Purcell spin echoes at 4T and 7T.** *Magn Reson Med* 2002;47:629–33